Hydrochemical changes induced by underground pumped storage hydropower and their associated impacts

Estanislao Pujades[1], Anna Jurado[1], Philippe Orban[1], Carlos Ayora[2], Angélique Poulain[3], Pascal Goderniaux[3], Serge Brouyère[1], Alain Dassargues[1]

[1] Hydrogeology and Environmental Geology, Geo3, Dpt ArGEnCo, Aquapole, University of Liege, 4000 Liege, Belgium

[2] GHS, Institute of Environmental Assessment & Water Research (IDAEA), CSIC, Jordi Girona 18-26, 08034 Barcelona, Spain

[3] Geology and Applied Geology, University of Mons, Mons, Belgium

Corresponding author: Estanislao Pujades

Phone: +3243663799

e-mail: estanislao.pujades@ulg.ac.be / estanislao.pujades@gmail.com

Abstract

Underground pumped storage hydropower (UPSH) using abandoned mines is an alternative system to manage electricity production in flat regions. Water from an underground reservoir is pumped to a surface reservoir to store electricity in the form of potential energy. Later, water is discharged through turbines into the underground reservoir to produce electricity when demand increases. During this operation, the water hydrochemistry continuously evolves. It varies in order to reach chemical equilibrium with the atmosphere (in the surface reservoir) and with the surrounding porous medium and groundwater (in the underground reservoir). The hydrochemical variations may lead to reactions in the reservoirs and in the surrounding porous medium, causing potentially negative consequences for the environment and the system efficiency, especially when pyrite is present in the surrounding porous medium. In this case, pyrite oxidation leads to a decrease in pH and the precipitation of goethite or schwertmannite in the surface reservoir. The decrease in pH is mitigated when calcite is present in the porous medium. However, other concerns may arise, such as slight increases in pH, the precipitation of ferrihydrite and calcite in the surface reservoir, and the oxidation of pyrite and dissolution of calcite in the surrounding porous medium. Understanding the pH variations and the precipitation/dissolution of minerals is of paramount importance in terms of the environmental impacts and system efficiency. For this reason, with numerical modelling, this work investigates the main hydrochemical changes and their associated consequences when abandoned deep mines are used for UPSH. The main objective is to highlight the importance of considering hydrochemical aspects when designing future UPSH plants.

Keywords: Energy Storage System, Reactive Transport Modelling, Deep Mine, Pyrite, Calcite.

1. Introduction

The main concern related to renewables energies, such as solar or wind energies, is that the electricity production is highly variable and cannot be adapted to the demand (Okazaki et al., 2015; Athari and Ardehali, 2016; Giordano et al., 2016; Hu et al., 2016; Mileva et al., 2016). This fact reduces their efficiency and limits their applicability. Energy storage systems (ESSs) are a solution to manage the variable electricity production of renewable sources and to increase the use of these sources (Gebretsadik et al., 2016). Such systems allow the storage of excess electricity generated during periods of low energy demand and the production of electricity when the demand increases (Delfanti et al., 2015; Mason, 2015). Pumped storage hydropower (PSH) is the most-used ESS (EPRI, 2010). It allows for the storage and production of a large amount of electricity (Steffen, 2012). PSH plants consist of two water reservoirs located at different elevations. The excess electricity is used to pump water from the lower to the upper reservoir, thus storing electricity in the form of potential energy. When the energy demand increases, water is discharged from the upper to the lower reservoir through turbines to produce electricity (Hadjipaschalis et al., 2009). Although PSH is widely used (Zhang et al., 2016), such systems are constrained by topographic aspects because the reservoirs must be located at different elevations, limiting the locations where plants can be constructed (Mueller et al., 2015). In addition, PSH is controversial regarding its impacts on the landscape, land use, environment (vegetation and wildlife) and society (relocations) (Wong, 1996; Kucukali, 2014). Consequently, new types of ESSs have been evoked as potential alternatives during the last years. One of them is the underground pumped storage hydropower (UPSH) (Uddin and Asce, 2003), where the lower reservoir is underground while the upper one is located at the surface (Barnes and Levine, 2011). UPSH has been considered and some projects have been planned in different parts of the world. However, there are no bibliographical evidence of constructed UPSH plants.

For instance, a project was started in the 1980s in the Netherlands, but the plant was eventually not installed for different reasons, such as unsuitable characteristics of the underground area (Spriet, 2014). Similarly, Wong (1996) proposed the installation of UPSH plants in Singapore using abandoned quarries as surface reservoirs and excavating the underground reservoirs. More recently, Severson (2011) suggested potential sites to establish a taconite mine in Minnesota (USA) and to use the excavated cavity after the mining activities as the underground reservoir for a UPSH plant. UPSH has also been investigated in Germany (Alvarado et al., 2016; Zillmann and Perau, 2015; Luick et al., 2012), Belgium (Spriet, 2014), Spain (Menéndez et al., 2017) and South Africa (Khan and Davidson, 2016; Winde et al., 2017).

The most important benefit of UPSH in comparison with PSH is that UPSH is not limited by the topography and could even be used in flat regions. Consequently, more possibilities exist to establish UPSH plants (Meyer, 2013). Impacts associated with landscape, land use and society (relocations) are lower than those of PSH because at least one of the reservoirs is located underground. Environmental impacts are different than those produced by PSH and must be evaluated carefully. In addition, re-used abandoned mines would provide added value to local communities after the cessation of mining activities.

The main concern regarding the use of abandoned mines is that mine walls are generally not waterproofed. Thus, UPSH plants interact with the surrounding porous medium exchanging water. To date, this interaction has only been studied from a flow point of view. Some studies have been focused on the impacts related to water exchange (1) on the piezometric head field (Pujades et al., 2016; Poulain et al., 2016; Bodeux et al., 2017) and (2) on the efficiency of the plant (Pujades et al., 2017a). However, there are no studies to date that have assessed the hydrochemical modifications induced by UPSH and its associated impacts on the environment and the efficiency. Induced hydrochemical

modifications have not been reported to date given that this is an emergent EES. In fact, as previously mentioned, there are no bibliographical evidence of operational UPSH plants. However, the chemical particularities of mine waters and their behaviour have been recognised as important challenges for the application of UPSH (EERA, 2016). In addition, similarities between UPSH and managed aquifer recharge, in which occurred hydrochemical changes are well known (Johnson et al., 1998; Barker et al., 2016; Antoniou et al., 2017), suggest that analogous changes may take place in UPSH systems. Obviously, the hydrochemical changes would be different since water is also pumped in UPSH and it reaches the surrounding porous geological medium through an underground cavity. For this reasons, it is meaningful to study the specific hydrochemical aspects associated to UPSH.

Under natural conditions, water in the underground reservoir and groundwater in the surrounding porous medium are in chemical equilibrium with the porous materials. Once the activity of the UPSH plants starts, water from the underground reservoir is pumped, discharged and stored in the surface reservoir. During this operation, water is aerated, and therefore, its chemical composition evolves to a new chemical equilibrium with the atmosphere. This is directly related to a variation in the dissolved O_2 and CO_2 concentrations. When this water is subsequently discharged from the surface to the underground reservoir, it evolves again towards another chemical equilibrium with the surrounding porous medium. This continuous evolution of the water chemistry may lead to the precipitation and dissolution of minerals, and their associated impacts such as variations in pH. For example, the oxidation of sulfides, which are common in coal-mined environments (Younger et al., 2002), would result in groundwater with a very low pH (Bigham and Nordstrom, 2000). As a result, the UPSH activity would possibly affect the surrounding groundwater quality. If part of the pumped water must be discharged in surface water bodies because groundwater inflows progressively fill the underground

cavity (Pujades et al., 2016; Bodeux et al., 2017), the quality of those water bodies could also be affected. These environmental issues are of paramount importance because future UPSH plants should respect the Water Framework Directive (WFD,2000/60/EC) to ensure a "good state" of water bodies, and especially groundwater, bodies. Hydrochemical changes are also relevant in terms of efficiency. Low pH values may accelerate the corrosion of equipment (pipes, pumps, turbines, concrete structures) (Kapil and Bhattacharyya; 2016; Sharma et al., 2011), whilst minerals precipitation may alter their mechanical efficiency (Sterpejkowicz-Wersocki, 2014). Thus, hydrochemical changes may lead to a decrease of efficiency and durability of the facilities. Moreover, periodical maintenance and cleaning tasks may be required.

For all these reasons, it is crucial to anticipate hydrochemical changes induced by UPSH and their consequences on the environment and the efficiency of the system. This issue is investigated in this work through numerical reactive transport models. The main reactive transport processes associated with the groundwater-UPSH water interactions are simulated considering three synthetic cases. The main objectives of this work are 1) to prove that UPSH activities can induce relevant hydrochemical changes, 2) to show that these changes may entail negative consequences for the environment and the efficiency of the system and 2) to highlight the importance of considering them in the design of future UPSH plants to ensure their feasibility.

2. Materials and methods

2.1. Problem statement

The problem is sketched schematically in Figure 1. An underground reservoir 50 m by 50 m on 10 m of height, located in an unconfined aquifer is considered. The top and bottom of the underground reservoir are at a depth of 95 and 105 m, respectively. The surrounding porous medium is 200 m thick, and the external boundaries are located 500

m away from the underground reservoir. In natural conditions groundwater flows from the western to the eastern boundary. The head is considered to be at depths of 92.5 and 97.5 m on the west and east boundaries, respectively. Under natural conditions, the water table is located just at the top of the underground reservoir (95 m depth), which is therefore totally saturated.

2.1.1. Chemistry of the porous medium

Abandoned coal mines are potential underground cavities to be used as underground reservoirs for constructing UPSH plants. Sulfide minerals, whose oxidation may entail important consequences for water chemistry, are common in coal deposits, and pyrite is usually the most common sulfide mineral in coal-mined environments (Akcil and Koldas, 2006). Thus, Hypothesis 1 (H1) considers that the geological medium contains 1% pyrite. The percentage of pyrite is not too much relevant since it is not totally consumed during the simulation time. Coal mine deposits surrounded by carbonates or containing lenses or intercalated layers of them have been worldwide reported (Sharma et al., 2013; Campaner et al., 2014; Xu et al., 2018) and carbonates counterbalance the negative effects produced by pyrite oxidation. For this reason, Hypothesis 2 (H2) considers that the geological medium contains 1% pyrite and 10% calcite. The percentage of calcite (carbonates) ensure that the neutralization acidic potential of the surrounding porous medium allows counterbalancing totally the effects of pyrite oxidation because the neutralization potential ratio is higher than 4 (Price et al., 1997). Hypotheses 1 and 2 represent the two boundary scenarios in which the neutralization capacity is null (H1) or total (H2). Results of intermediate scenarios, in which the carbonate/pyrite ratio is lower than that considered in H2, would be comprehended by those obtained for hypotheses H1 and H2. Finally, the presence of only calcite (10%) is considered in Hypothesis 3 (H3) for two reasons. On the one hand, limestone mines are also considered

to be used as underground reservoirs for UPSH and these mines can be also underground as shown the literature (Koch, 1987; Hustrulid et al., 2001). On the other hand, the expected behaviour is very different to that occuring when pyrite is present. Note that these percentages refer to the initial concentrations, and the conditions will evolve depending on the reactions that occur. It is assumed that the rest of the porous medium is made up of silicates, whose reaction rates are very slow (White and Brantley, 1995) and can be neglected. Silicate dissolution and ion exchange is possible (Johnson et al., 1999) and should be considered in some situations, as this has been proved in works developed in the field of aquifer managed recharge. However, the objective of this work is to establish the main trends and highlight the importance of considering the hydrochemistry in the design of future UPSH plants. For this reason, only minerals (pyrite and calcite) whose behavior is well known are selected. Obviously, the composition of the geological medium in real cases is much more complex, and preliminary studies performed before constructing UPSH plants must consider all the existing minerals and all the processes.

2.1.2. Pumping and discharging frequencies

The actual pumping and discharging frequency cannot be forecasted. This depends on numerous factors such as the day, season, meteorology, electrical smart grid, optimization scenarios or economic issues. Therefore, at this stage, representative results are obtained assuming day/night cycles of 12 hours (i.e., water is pumped for 12 hours and discharged during the next 12 hours). The underground reservoir is considered almost empty and almost full after each pumping/discharging phase. Thus, given the dimensions of the underground reservoir, pumping/discharging rates are chosen to be 43,000 m^3/d. Note that the underground reservoir is not totally emptied at the end of each cycle. A residual water depth of 1.4 m is intentionally left in the reservoir to keep nodes

from which water is pumped and injected in a fully saturated zone. Appendix A shows the results of a sensitivity analysis in which the pumping/discharging rate is reduced by half.

2.2. Basic concepts

The most relevant reactions that occur in the modelled hypotheses and their consequences are summarized in this section. Water aeration occurs each time that water is discharged and stored in the surface reservoir. This process induces CO_2 and O_2 exchanges between the water and the atmosphere. Thus,

$$CO_2(aq)=CO_2(g) \quad \text{(R1)}$$

$$O_2(aq)=O_2(g) \quad \text{(R2)}$$

The presence of pyrite is assumed in the H1 and H2 hypotheses. When the O_2 concentration in the water increases as a consequence of R2, pyrite is oxidized and ferrihydrite may precipitate as follows:

$$FeS_2+15/4\,O_2(aq)+7/2\,H_2O=Fe(OH)_3(s)+2SO_4^{2-}+4H^+ \quad \text{(R3)}$$

Ferrihydrite ($\approx Fe(OH)_3$) precipitation induced by reaction R3 occurs if the water pH is higher than 6. Other minerals precipitate because of pyrite oxidation at low pH ranges. Goethite ($FeOOH+3H^+$) may precipitate between pH 4 and pH 6, whilst schwertmannite ($Fe_8O_8(OH)_{4.5}(SO_4)_{1.75}$) may precipitate at pH values lower than 4 (Sánchez-España et al., 2011). Goethite and schwertmannite precipitate as follows:

$$Fe^{3+}+2H_2O = FeOOH+3H^+ \quad \text{(R4)}$$

$$8Fe^{3+}+12.5H_2O+1.75SO_4^{2-}=Fe_8O_8(OH)_{4.5}(SO_4)_{1.75}+20.5H^+ \quad \text{(R5)}$$

The common characteristic of these three reactions is that they reduce the pH. These reactions are characteristic of acid mine drainage processes (Banks et al., 1997; Robb, 1994). Pyrite oxidation in the numerical model is calculated using the kinetic law

described by Williamson and Rimstidt (1994) and considering a specific surface area of 1000 m^{-1}.

Calcite in the surrounding porous medium is considered for the H2 and H3 hypotheses. In this case, the following reaction occurs:

$$CaCO_3 + 2H^+ = Ca^{2+} + CO_2(aq) \quad \text{(R6)}$$

R6 does not occur in a unidirectional way, and if the pCO_2 is modified, calcite may precipitate or be dissolved. For example, surface aeration of the pumped water induces a reduction of pCO_2, and, as a result, calcite should precipitate. The kinetics of calcite are implemented in the model using the kinetic law defined by Plummer et al. (1978) and considering a specific surface area of 45.3 m^{-1}. Thermodynamic data for aqueous speciation and mineral and gas solubility are taken from the Wateq database, as implemented in the PHREEQC code (Parkhurst and Appelo, 1999). The solubility constant of schwertmannite is taken from Sánchez-España et al. (2011).

Under the H1 hypothesis, the aeration of the water pumped into the surface reservoir would increase the pO_2. When this water is discharged into the underground reservoir, it oxidizes pyrite and reduces the pH. In addition, when the water is stored in the surface reservoir, ferrihydrite, goethite or schwertmannite precipitate. In H2, pyrite oxidation would induce the dissolution of calcite, which acts as a buffer, preventing a decrease in pH. On the other hand, under the H2 and H3 hypotheses, the decrease in pCO_2 in the surface reservoir could produce calcite precipitation. Note that, UPSH plants may act as CO_2 sources because pCO_2 increases each time that water is discharged into the underground reservoir. Therefore, CO_2 emission is quantified under the H2 and H3 hypotheses. The influence of the specific surface area is assessed in a sensitivity analysis whose results are shown in the Appendix A.

2.3. Numerical model

The problem was simulated using the code PHAST (Parkhurst et al., 1995; Parkhurst and Kipp, 2002). This code solves multicomponent, reactive solute transport in three-dimensional saturated groundwater flow (Parkhurst et al., 2010). Geochemical reactions are solved by the code PHREEQC (Parkhurst, 1995; Parkhurst and Appelo, 1999). Flow and transport are computed with a modified version of HST3D (Kipp, 1987, 1997). It is possible to identify a line of symmetry crossing the domain from the west to the east boundary located just in the centre of the considered problem crossing the domain from the west to the east boundary (Figure 1 and Figure 2a). Therefore, the problem can be simplified by taking advantage of this symmetry, and only a half of the domain is modelled (Figure 2a). This simplification does not affect the results and allows reducing the computation times. The modelled domain is divided into 15600 elements refined in and around the underground reservoir (Figure 2b). The size of the elements ranges from 2 to 100 m.

The flow and transport parameters are the same for the three hypotheses. For the porous medium, the hydraulic conductivity (K) and storage coefficient (S) are chosen as 0.01 m/d and 0.05, respectively. The longitudinal (α_L) and transversal (α_L) dispersivities are assumed to be 10 and 1 m, respectively. The underground reservoir (i.e., cavity) is modelled by adopting a high value of K (10^6 m/d), S of 1, and a dispersivity of 10^4 m in the three directions. This value of dispersivity means that mixing of the discharged water in the underground reservoir is rapid and homogeneous. This assumption is acceptable because a large volume of water is discharged within a short period of time facilitating the mixing. Note that the influence of the dispersivity used to simulate the underground reservoir has been previously evaluated and is considered negligible (Pujades et al., 2017b).

2.3.1 Flow boundary conditions (BCs)

Dirichlet boundary conditions (BCs) are adopted at the western and eastern boundaries. An initial hydraulic gradient of 0.005 is modelled by prescribing the piezometric head at a depth of 92.5 and 97.5 m on the western and eastern boundaries, respectively. Pumping and discharging rates of 21,500 m^3/d are simulated by prescribing Neumann BCs in nodes located at the base of the underground reservoir. This rate allows for the dewatering and filling of 8.6 m of the cavity in half a day. Note that the prescribed flow rates are half those mentioned above because only half of the problem is modelled. Recharge through the upper and lower boundaries of the model is not considered and a no-flow condition is assumed.

2.3.2 Hydrochemical conditions and transport boundary conditions

The initial hydrochemical conditions and transport boundary conditions are chosen according to the hypotheses considered (H1, H2 or H3). Groundwater that 1) is initially present in the whole modelled domain, (i.e., in the underground reservoir and in the surrounding porous medium), 2) enters through the west boundary (during all the simulated time), and 3) initially flows out through the east domain, is in equilibrium with pyrite in H1, with pyrite and calcite in H2 and with calcite in H3. In addition, it is prescribed that groundwater under natural conditions has a CO_2 partial pressure (pCO_2) of 10^{-2} atm in H2 and H3. This value is chosen according to the literature (Faimon et al., 2012; Sanz et al., 2011). Note that CO_2 is not considered under hypothesis H1 because it is not relevant for the expected reactions.

2.3.3 Simulation strategy

The most challenging aspect of the numerical model is to simulate the evolving hydrochemistry of the discharged water during successive pumping/discharging cycles. The hydrochemistry of discharged water results in its aeration in the surface reservoir but

also depends on the chemical composition of the previously pumped water, which cannot be predicted in advance. To address this issue and to model the problem in a suitable manner, successive iterations progressively increasing the final simulated time are performed. The characteristics of the discharged water obtained from the previous iteration results are re-introduced at each iteration. The simulations are performed using the following steps:

1. A first iteration of 0.5 days is performed. The results of this iteration provide the hydrochemistry of water pumped to the surface reservoir from 0 to 0.5 days.
2. With the results of the first iteration, the second iteration from 0 to 1.5 days can be carried out. The input files of the model regarding the hydrochemistry of the discharged water from 0.5 to 1 day are actualized using the characteristics of the previously pumped water (from 0 to 0.5 day) and considering two different scenarios (Sce1 and Sce2). In Sce1, it is assumed that water in the surface reservoir reaches chemical equilibrium with the atmospheric O_2 and CO_2. Thus, the partial pressures of O_2 (pO_2) and pCO_2 of the stored water in the surface reservoir reach $10^{-0.7}$ and $10^{-3.5}$ bar, respectively, before being discharged in the underground reservoir. In Sce2, it is considered that stored water in the surface reservoir does not reach complete chemical equilibrium with the atmospheric O_2 and CO_2. It is assumed that the pO_2 and pCO_2 of the stored water in the surface reservoir are 10^{-1} and $10^{-2.29}$ bar, respectively, before being discharged. These two partial pressure values correspond to half of the O_2 and CO_2 concentrations if a chemical equilibrium with the atmosphere is fully achieved. These two scenarios are helpful to evaluate the role of the pumping/discharging frequency on the hydrochemical changes. In addition, it is assumed that the

precipitation of calcite, ferrihydrite, goethite and/or schwertmannite in the surface reservoir occurs at equilibrium. This second iteration (from 0 to 1.5 day) provides the hydrochemistry of the pumped water from 1 to 1.5 day.

3. The same process as in the previous step is followed. Thus, using the results of the previous iteration, the model is simulated from 0 to 2.5 days. Now, the hydrochemistry of the pumped water from 1 to 1.5 days is used to define the discharged water from 1.5 to 2 days. In this case, Sce1 and Sce2 are also considered.
4. Subsequently, the fourth iteration from 0 to 3.5 days is performed using the characteristics of the pumped water from 2 to 2.5 day, on so on.

Note that each iteration is started at time 0, which increases the computation time. Obviously, attempts are made to restart each simulation at the end of the previous one. However, this was not possible due to limitations of the used code. In total, 30 days were simulated because this methodology requires a long computation time (more than two weeks are needed to simulate 30 days, and the computation time increases exponentially with the simulated time). Nevertheless, 30 days are enough to reach the main objectives of evaluating the main hydrochemical reactions and their consequences in UPSH plants. A simple code using Python (Van Rossum and Drake, 2011) was built to automate the process and facilitate the tasks. The code reads the results of each iteration, updates the input files and initiates the subsequent iteration.

3. Results and discussion

3.1. pH evolution

3.1.1. Hypothesis 1 (only pyrite)

Figure 3a shows the calculated pH evolution in the surface and underground reservoirs and in the surrounding porous medium (at 5 and 15 m from the underground

356 reservoir in the downgradient direction). Figure 3a displays the numerical results for Sce1
357 (i.e., a chemical equilibrium with atmospheric O_2 is reached in the surface reservoir) on
358 the left, and for Sce2 (i.e., a chemical equilibrium with atmospheric O_2 is not totally
359 reached in the surface reservoir) on the right. In the case of Sce1, the pH values in the
360 reservoirs decrease abruptly during the first cycles. Then, the decrease in pH becomes
361 more moderate. This behaviour is consistent with the expected reactions since the
362 increment of pO_2 in the surface reservoir promotes pyrite oxidation when the water is
363 again discharged into the underground reservoir. The pH values are around 3 in the
364 underground and surface reservoirs at the end of the 30-day simulation time. The pH
365 values in the surrounding porous medium at 5 m from the underground reservoir also
366 decrease as a consequence of groundwater exchanges and pyrite oxidation. The
367 decreasing trend in the pH values is similarly to that seen for the pH in the underground
368 reservoir. The decrease depends on the distance from the cavity and there is a delay for
369 larger distances. The pH decrease is less abrupt and lower at 15 m. At the end of the
370 simulation time, the pH values are 3.2 and 4.4 at 5 and 15 m, respectively. O_2 is totally
371 consumed by pyrite oxidation each time that water is discharged. This means that water
372 aeration implies a continuous injection of O_2. Consequently, the pH is expected to
373 decrease until pyrite is totally consumed. In the case of Sce2, the pH evolution is similar
374 to that for Sce1, but the pH values are slightly higher. The pH values at the end of the
375 simulation are 3 in the underground reservoir, 3.2 in the surface reservoir, 3.3 at 5 m and
376 4.6 at 15 m from the underground reservoir. The computed pH distribution in the
377 surrounding porous medium after 5, 15 and 30 days is shown in Figure A1 of Appendix
378 B.
379
380 *3.1.2. Hypothesis 2*

Figure 3b shows the calculated pH evolution in the surface and underground reservoirs and in the surrounding porous medium (5 and 15 m away from the underground reservoir in the downgradient direction) for Sce1 (on the left) and Sce2 (on the right) under hypothesis H2. In the case of Sce1, the pH values do not decrease like they do in H1 because calcite acts as a buffer. In fact, the pH increases instantaneously in the surface reservoir because the CO_2 exsolves. Note that the instantaneous increase is not observed in the figure because, prior to the first pumping, the surface reservoir is assumed empty. However, it does occur since the groundwater pH before the first pumping is 7.3. The pH in the underground reservoir also increases during the early cycles because this reservoir is filled with water from the surface one. After 2 days, however, the pH oscillates for each simulated cycle, and the pH decreases during discharging and increases during pumping periods. Discharged water has higher O_2 concentrations that are rapidly consumed by pyrite oxidation, thus promoting a decrease in the pH in the underground reservoir. When water is pumped, groundwater with higher pH values from the porous medium enters the underground reservoir and increases the pH. The pH values in the surrounding porous medium also increase during the simulation. The increase rate decay with time at 5 m and, at the end of the simulation, the pH is quasi-stable. The pH behaviour is similar for Sce2 (Figure 3b on the right). In this case, the initial increase in pH and oscillations in the underground reservoir are less intense because less CO_2 and O_2 are exchanged with the atmosphere. For both scenarios, the pH increase at 15 m from the underground reservoir is not appreciable in the figure. The distribution of the pH values in the surrounding porous medium after 5, 15 and 30 days is shown in Figure A2 of Appendix B.

3.1.3. Hypothesis 3

406 Figure 3c shows the pH evolution in the surface and the underground reservoirs
407 and in the surrounding porous medium (at 5 and 15 m from the underground reservoir in
408 the downgradient direction) for Sce1 (on the left) and Sce2 (on the right) under hypothesis
409 H3. In the case of Sce1, the pH values do not decrease since this hypothesis does not
410 consider the presence of pyrite. In this case, pH increases instantaneously in the surface
411 reservoir and then remains constant. As in hypothesis H2, an instantaneous increase is
412 not observed in the figure because, prior to the first pumping, the surface reservoir is
413 assumed emptied. However, it occurs since the groundwater pH before the first pumping
414 is 7.3. The pH value also increases in the underground reservoir because it is filled with
415 water from the surface reservoir. The increase is less extreme in the underground
416 reservoir since the discharged water is mixed with the groundwater of the surrounding
417 porous medium. The pH also increases in the surrounding porous medium, but it depends
418 on the distance from the underground reservoir. The increase in pH is less as the distance
419 increases, and at a distance of 15 m from the underground reservoir, the observed pH
420 variation is negligible over the simulated time. The system behaves in a similar way when
421 Sce2 is considered (Figure 3c on the right) but the maximum pH values are lower. If less
422 CO_2 is exchanged with the atmosphere in the surface reservoir, pH variations are smaller.
423 Oscillations in the pH value are observed in the underground reservoir. Each time that
424 water is pumped, groundwater from the surrounding porous medium enters the
425 underground reservoir. Given that the pH in the surrounding porous medium is slightly
426 lower, groundwater inflows cause a decrease in the pH inside the underground reservoir.
427 Similarly, each time that the underground reservoir is filled, water with a low pCO_2 and
428 high pH enters the porous medium and mixes with the groundwater, which increases the
429 pH values around the underground reservoir. The pH distribution in the surrounding
430 porous medium after 5, 15 and 30 days is shown in Figure A3 of Appendix B.
431

3.2. Precipitation, dissolution and oxidation of minerals

3.2.1. Hypothesis 1

Figure 4a shows the mass of goethite and schwertmannite precipitated in the surface reservoir for Sce1 (on the left) and Sce2 (on the right) under hypothesis H1. Ferrihydrite does not precipitate because the pH is lower than 6, and goethite only precipitates during the first cycles in which pH values range from 4 to 6. During the subsequent cycles, the pH is lower than 4, and only schwertmannite precipitates. The results for Sce1 and Sce2 are slightly different. On the one hand, the amount of precipitated goethite is lower in Sce1 because it only precipitates during two cycles whilst goethite precipitates during the three first cycles in Sce2. On the other hand, more schwertmannite precipitates in Sce1 because more pyrite is dissolved in the surrounding medium, and therefore, more minerals are available to precipitate. Minerals neither precipitate in the porous medium nor in the underground reservoir. Figure 5a shows the evolution of pyrite in the porous medium 5 m from the underground reservoir for Sce1 and Sce2 under hypothesis H1. The percentage of pyrite in the porous medium decreases for both scenarios because of its oxidation. However, the oxidation rate is higher in Sce1 because more O_2 is added to the system in the surface reservoir.

3.2.2. Hypothesis 2

Figure 4b shows the precipitated mass of calcite and ferrihydrite in the surface reservoir for Sce1 (on the left) and Sce2 (on the right) under hypothesis H2. In this case, ferrihydrite precipitates instead of goethite and of schwertmannite because the pH is higher than 6. The precipitation rate of calcite is much higher during the early cycles than in the later ones. However, the precipitation rate of ferrihydrite is apparently constant, except during the initial cycles. The mass of precipitated calcite is higher than the mass

457 of ferrihydrite at the end of the simulations and the scenarios (Sce1 and Sce2) differ in
458 the total precipitated mass of both minerals, but not in the global trends.

459 Figure 5b displays the evolution of calcite and pyrite concentrations at a distance
460 of 5 m from the underground reservoir for Sce1 and Sce2 under hypothesis H2. Calcite
461 and pyrite are continuously dissolved or oxidized in the surrounding porous medium. As
462 a result, their percentages in the surrounding porous medium decrease. The dissolved
463 and oxidized masses are higher for Sce1, especially for calcite. The dissolution and
464 oxidation decrease significantly when the atmosphere-water equilibrium is not considered
465 (Sce2). In this case, the pO_2 in the discharged water is lower, and less pyrite and calcite
466 are oxidized and dissolved, respectively.

467 Note that the maximum precipitation rates of calcite are observed during early
468 cycles. At the beginning, all pumped water is equilibrated with the calcite of the porous
469 medium and has a pCO_2 of 10^{-2}. As a result, a large decrease in the CO_2 in the surface
470 reservoir occurs, and the associated precipitations are high. In contrast, after some
471 cycles, the pCO_2, and therefore, the mass of precipitated calcite in the surface reservoir,
472 are lower because the discharged water (low pCO_2) fills the underground reservoir and
473 only the water exchanges with the surrounding medium introduce new CO_2 in the pumped
474 water.

475

476 *3.2.3. Hypothesis 3*

477 Figure 4c displays the mass of precipitated calcite in the surface reservoir for Sce1
478 (on the left) and Sce2 (on the right) under hypothesis H3. The precipitation rate of calcite
479 is higher during the early cycles than during the later ones. The decrease in the
480 precipitation rate occurs during the first 5 days, and after, it is apparently constant.
481 Obviously, if the exchange of CO_2 with the atmosphere is lower (Sce2), calcite
482 precipitation decreases. When the discharged water is exchanged with the surrounding

porous medium and mixed with groundwater, its pCO_2 increases, and the pH decreases, which promotes calcite dissolution. This fact is corroborated by the results. The pH values in the surrounding porous medium are always lower than those in the surface and underground reservoirs (Figure 3c), while the mass of calcite decreases in the surrounding porous medium (Figure 5c). Figure 5c displays the evolution of the calcite percentage in the surrounding porous medium 5 m away from the underground reservoir. Calcite is dissolved during all simulation times. The dissolution rate is higher at the beginning, and after 4-5 days, it decreases and becomes nearly constant. Because less CO_2 is exchanged with the atmosphere for Sce2, the dissolved calcite is also lower. Note that, as in the previous hypothesis, the maximum precipitation and dissolution rates are observed during early times. On the one hand, the variation of the pCO_2 in the surface reservoir is higher at the beginning than at the later simulated times. On the other hand, the contrast between the discharged water and groundwater is high during early cycles, promoting the dissolution of calcite and its associated precipitation in the surface reservoir.

3.3. Assessment of environmental impacts and efficiency

One of the objectives of the numerical modelling may be to inform about the environmental impacts identified in specific sites. Unfortunately, as mentioned above, there are no bibliographical evidence of constructed UPSH plants. It is thus an emergent technology, and therefore, environmental impacts have not been reported to date. In this case, numerical modelling is used for predicting the potential environmental impacts of UPSH, highlight their importance and raise awareness about the necessity of considering them for designing future UPSH plants. In addition, it allows deducing if UPSH related activities may induce difficulties in the compliance of the Water Framework Directive (WFD,2000/60/EC). This directive specifies that the states must prevent the deterioration

of groundwater and surface water bodies. The environmental objectives may be lowered if the water bodies are affected by human activities with an important socio-economic component, as it could be for UPSH plants. Even so, in these situations, the states must guarantee the highest ecological and chemical status possible for surface water bodies and the least possible changes for groundwater bodies. The results show that UPSH activity may alter the chemical properties of groundwater and surface water (when water is discharged into surface water bodies), especially if pyrite is present in the geological formations. For this reason, hydrochemical impacts must be assessed prior the construction of UPSH plants to ensure that the Water Framework Directive would still be respected in the future. More specifically, in H1, pyrite oxidation leads to low pH values, and the pH increases in H2 and H3. In H2, calcite dissolution mitigates the pH decrease induced by pyrite oxidation, and only a slightly increase in pH is observed when the pCO_2 decreases in the surface reservoir to achieve equilibrium with the atmosphere. This is the same process that explains the pH increase observed for H3. The main difference between H2 and H3 is that, after an early increase in pH, it decreases gradually for H2 while remaining constant for H3. pH variations occur also in both reservoirs, which is of paramount importance in environmental terms because the excess stored water in the surface reservoir may have to be discharged into surface water bodies, thus also modifying their pH values.

The porosity in the surrounding porous medium increases as a result of the dissolution of calcite and the oxidation of pyrite. The porosity increases $2.2 \cdot 10^{-5}$ and $1 \cdot 10^{-5}$ % for Sce1 and Sce2 under hypothesis H1, $1.4 \cdot 10^{-4}$ and $4.2 \cdot 10^{-5}$ % for Sce1 and Sce2 under hypothesis H2, and $3.7 \cdot 10^{-5}$ and $3.9 \cdot 10^{-6}$ % for Sce1 and Sce2 under hypothesis H3, respectively. The porosity increases more for H2 because pyrite is oxidized and calcite is dissolved at the same time. Although the increase in porosity is not relevant during the simulated period, it should be considered for large activity periods. The

groundwater exchanges, and thus the potential environmental impacts, increase with higher porosities (Pujades et al., 2016). In addition, if a pollutant was accidentally discharged into the surface reservoir, it would reach faster the subsurface environment.

Table 1 summarizes the released CO_2 (g/kWh) for both scenarios (Sce1 and Sce2) under hypotheses H2 and H3. Emissions are computed considering the total CO_2 released during the total simulated period, and the volume of released CO_2 once the emission rates are stabilized after some days of activity (≈10 days). The results show that UPSH plants may act as a CO_2 source when carbonates are present in the surrounding porous medium. However, the emissions are much lower than those produced by other energy sources such as coal or gas (Schlömer et al., 2014).

The results are also relevant in terms of efficiency. Low pH values in the reservoirs may lead to the corrosion of UPSH facilities, and the precipitation of minerals may induce clogging events (e.g., in pipes). As a result, maintenance and cleaning tasks and the adequate selection of materials are needed to avoid corrosion and clogging, to extend the useful life and to maximize the efficiency of the facilities (pumps, turbines, pipes). The dissolution and oxidation of minerals in the surrounding porous medium are also relevant in terms of energy production because the efficiency of pumps and turbines depends on groundwater exchanges (Pujades et al., 2017a). Generally, their efficiency increases with greater water exchanges. The results show that the increase in porosity, and thus in groundwater exchanges, is low over short periods. However, this increase should be investigated because the useful life of future UPSH plants is expected to be longer.

When equilibrium between the atmosphere and water from the surface reservoir in not completely reached, the behaviour of the system is similar. However, the pH variations and the masses of minerals dissolved, oxidized and precipitated are lower. Therefore, the comparison between Sce1 and Sce2 (for the three hypotheses) reveals

560 that impacts on the environment and system efficiency are smaller as the aeration during
561 the discharge and storage of water in the surface reservoir is less important.
562
563 **5. Conclusions and prospects**
564 Induced hydrochemical reactions result from the surface exposure of the pumped
565 water in UPSH contexts. When water is discharged and stored in the surface reservoir,
566 the concentrations of O_2 and CO_2 evolve to reach chemical equilibrium with the
567 atmosphere. Thus, O_2 tends to increase, and CO_2 to decrease. In addition to the reactions
568 occurring in the surface reservoir, when water is discharged into the underground
569 reservoir, it interacts with the groundwater and the surrounding porous medium. This
570 interaction also leads to chemical reactions.
571 The impacts are especially relevant if pyrite is present in the porous medium. The
572 increase in the pO_2 induces pyrite oxidation. This reaction releases H^+, decreasing the
573 pH, which is relevant in terms of environmental impacts and efficiency of UPSH plants.
574 Lower pH values may lead to the corrosion of the facilities (pipes, pumps and turbines).
575 In addition, ferrihydrite, goethite or schwertmannite may precipitate in the surface
576 reservoir requiring maintenance and cleaning tasks.
577 pH does not decrease when calcite is present in the porous medium. In contrast,
578 the pH slightly increases. However, other aspects must be regarded, such as the
579 precipitation of calcite and ferrihydrite in the surface reservoir. In addition, a small amount
580 of CO_2 is released to the atmosphere..
581 The results also show that UPSH may induce the dissolution/oxidation of minerals
582 in the porous medium. This fact may be relevant in terms of efficiency and environmental
583 impacts. The dissolution and/or oxidation of minerals promotes the increase of the
584 transmissivity and/or the porosity. Consequently, water exchanges between the
585 surrounding porous medium and the underground reservoir would increase.

A comparison of the numerical results obtained for Sce1 and Sce2 reveals that the hydrochemical changes induced by UPSH and their associated consequences decrease 1) when the water is stored in the surface reservoir over a shorter period and 2) when the aeration, occurred when pumped water is discharged and stored into the surface reservoir, is lower. Thus, the pumping/discharging frequency and the method to discharge and to store the pumped water in the surface reservoir determine the reactions and their associated impacts.

It was not possible to lengthen the simulation periods because of the long computation times required. Although an attempt was made to modify the simulation strategy and start each iteration at the end of the previous one, it was ultimately not possible. However, the simulated period is sufficient to identify the main trends of the system, the reactions that occur and their consequences. It is possible to affirm that after a long active period of a UPSH plant, all the pyrite near the underground reservoir would be oxidized. However, the pH would continue to decrease in the surrounding porous medium because the discharged water with high concentrations of O_2 would reach downstream areas in which pyrite would still be present. The only difference would be noted in the amounts of precipitated ferrihydrite, goethite and schwertmannite. The products of the oxidized pyrite far from the underground reservoir could not be mobilized by the pumping. Similar predictions could be done for contexts in which calcite is present.

This work highlights the importance of considering hydrochemical aspects for the construction of future UPSH plants. In fact, preliminary studies focused on determining the hydrochemical changes and their consequences should be mandatory. The results of these preliminary studies combined with the environmental policies will allow taking decisions concerning the construction of UPSH plants using abandoned mines. In other words, these preliminary studies should be considered for selection of the potential abandoned mines to be used as underground reservoirs. Preliminary studies must consist

612 in a detailed hydraulic and hydrochemical characterization of the geological medium by
613 means of field tests (pumping and tracer tests), mineralogical analyses and laboratoty
614 tests. In addition, the main characteristics of the plant (volume of the underground
615 reservoir, flow-rates, pumping/discharging frequencies, etc) must be considered and the
616 aeration process in the surface reservoir must be investigated to precisely quantify the
617 gas exchanges. All these informations should be integrated into reactive transport models
618 for predicting the consequences of reactive transport processes induced by UPSH.
619 Monitoring will be also needed during the operational phase of UPSH plants to verify that
620 hydrochemistry evolves as expected. In this context, hydrologists may play a specific role
621 during the selection, design and operational phases. Hydro(geo)logists should 1)
622 contribute in the characterization of the porous medium, 2) built the numerical models
623 and analyse the results, 3) design the monitoring strategies and monitor the system
624 evolution during the operational phase, and 4) establish guidelines for the selection of
625 potential sites for constructing UPSH plants.

626 The main difficulty faced with numerical models is ascertaining the characteristics
627 of the discharged water during each cycle. This problem can be addressed by using the
628 same modelling methodology proposed in this work. It consists of successive runs for
629 which the maximum simulation time is progressively increased. After each pumping
630 phase, the calculation is stopped, and the results are used to define the hydrochemical
631 features of the subsequently discharged water.

632 This work considers three simplified hypothesis with respect the chemical
633 composition of the porous medium. Obviously, hydrochemical changes induced by real
634 UPSH plants will be different and will vary for each specific site because they depend on
635 the chemical composition of the medium surrounding the underground reservoir.
636 However, this work aims to highlight that the hydrochemical changes may be relevant.
637 This is the proof that they may seriously impact the environment and the efficiency of the

638 UPSH plants. In fact, if they are not properly considered, they could put at risk the whole
639 feasibility of future UPSH plants.
640
641 **6. Acknowledgements**
642 E. Pujades and A. Jurado gratefully acknowledges the financial support from the
643 University of Liège and the EU through the Marie Curie BeIPD-COFUND postdoctoral
644 fellowship programme (2014-2016 and 2015-2017 “Fellows from FP7-MSCA-COFUND,
645 600405”). This research was supported by the Public Service of Wallonia – Department
646 of Energy and Sustainable Building through the Smartwater project.

References

Akcil, A., Koldas, S., 2006. Acid Mine Drainage (AMD): causes, treatment and case studies. Journal of Cleaner Production, Improving Environmental, Economic and Ethical Performance in the Mining Industry. Part 2. Life cycle and process analysis and technical issuesImproving Environmental, Economic and Ethical Performance in the Mining Industry. Part 2. Life cycle and process analysis and technical issues 14, 1139–1145. doi:10.1016/j.jclepro.2004.09.006

Alvarado, R., Niemann, A., Wortberg, T., 2016. Underground Pumped-Storage Hydroelectricity using existing Coal Mining Infrastructure. E-proceedings of the 36th IAHR World Congress.

Antoniou, A., Smits, F. and Stuyfzand, P., 2017. Quality assessment of deep-well recharge applications in the Netherlands. *Water Science and Technology: Water Supply*, *17*(5), pp.1201-1211

Athari, M.H., Ardehali, M.M., 2016. Operational performance of energy storage as function of electricity prices for on-grid hybrid renewable energy system by optimized fuzzy logic controller. Renewable Energy 85, 890–902. doi:10.1016/j.renene.2015.07.055

Banks, D., Younger, P.L., Arnesen, R.-T., Iversen, E.R., Banks, S.B., 1997. Mine-water chemistry: the good, the bad and the ugly. Environmental Geology 32, 157–174. doi:10.1007/s002540050204

Barker, J.L., Hassan, M.M., Sultana, S., Ahmed, K.M. and Robinson, C.E., 2016. Numerical evaluation of community-scale aquifer storage, transfer and recovery technology: A case study from coastal Bangladesh. *Journal of Hydrology*, *540*, pp.861-872

Barnes, F.S., Levine, J.G., 2011. Large Energy Storage Systems Handbook [WWW Document]. CRC Press. URL https://www.crcpress.com/Large-Energy-Storage-Systems-Handbook/Barnes-Levine/p/book/9781420086003 (accessed 3.12.17).

Bigham, J.M., Nordstrom, D.K., 2000. Iron and Aluminum Hydroxysulfates from Acid Sulfate Waters. Reviews in Mineralogy and Geochemistry 40, 351–403. doi:10.2138/rmg.2000.40.7

Bodeux, S., Pujades, E., Orban, P., Brouyère, S., Dassargues, A., 2017. Interactions between groundwater and the cavity of an old slate mine used as lower reservoir of an UPSH (Underground Pumped Storage Hydroelectricity): A modelling approach. Engineering Geology 217, 71–80. doi:10.1016/j.enggeo.2016.12.007

Campaner, V.P., Luiz-Silva, W. and Machado, W., 2014. Geochemistry of acid mine drainage from a coal mining area and processes controlling metal attenuation in stream waters, southern Brazil. *Anais da Academia Brasileira de Ciências*, *86*(2), pp.539-554.

Delfanti, M., Falabretti, D., Merlo, M., 2015. Energy storage for PV power plant dispatching. Renewable Energy 80, 61–72. doi:10.1016/j.renene.2015.01.047

European Energy Research Alliance (EERA), 2016. Underground Pumped hydro storage. EERA Joint Program SP4 – Mechanical Storage. Fact Sheet x. https://eera-es.eu/wp-content/uploads/2016/03/EERA_Factsheet_Underground-Pumped-Hydro-Energy-Storage_not-final.pdf

EPRI, 2010. Electric Energy Storage Technology Options: A White Paper Primer on Applications, Costs, and Benefits. Palo Alto, CA. 1020676.

Faimon, J., Ličbinská, M., Zajíček, P., Sracek, O., 2012. Partial pressures of CO2 in epikarstic zone deduced from hydrogeochemistry of permanent drips, the Moravian Karst, Czech Republic. Acta Carsologica 41. doi:10.3986/ac.v41i1.47

Gebretsadik, Y., Fant, C., Strzepek, K., Arndt, C., 2016. Optimized reservoir operation model of regional wind and hydro power integration case study: Zambezi basin and South Africa. Applied Energy 161, 574–582. doi:10.1016/j.apenergy.2015.09.077

Giordano, N., Comina, C., Mandrone, G., Cagni, A., 2016. Borehole thermal energy storage (BTES). First results from the injection phase of a living lab in Torino (NW Italy). Renewable Energy 86, 993–1008. doi:10.1016/j.renene.2015.08.052

Hadjipaschalis, I., Poullikkas, A., Efthimiou, V., 2009. Overview of current and future energy storage technologies for electric power applications. Renewable and Sustainable Energy Reviews 13, 1513–1522. doi:10.1016/j.rser.2008.09.028

Hu, Y., Bie, Z., Ding, T., Lin, Y., 2016. An NSGA-II based multi-objective optimization for combined gas and electricity network expansion planning. Applied Energy 167, 280–293. doi:10.1016/j.apenergy.2015.10.148

Hustrulid, W.A., Hustrulid, W.A. and Bullock, R.C. eds., 2001. *Underground mining methods: Engineering fundamentals and international case studies*. SME.

Johnson, J.S., Baker, L.A. and Fox, P., 1999. Geochemical transformations during artificial groundwater recharge: soil–water interactions of inorganic constituents. *Water research*, *33*(1), pp.196-206.

714 Kapil, N., Bhattacharyya, K.G., 2016. A comparison of neutralization efficiency of
715 chemicals with respect to acidic Kopili River water. Appl Water Sci 1–6.
716 doi:10.1007/s13201-016-0391-6
717 Khan, S.Y., Davidson, I., 2016. Underground Pumped Hydroelectric Energy Storage in
718 South Africa using Aquifers and Existing Infrastructure [WWW Document].
719 ResearchGate. URL
720 https://www.researchgate.net/publication/308780409_Underground_Pumped_Hy
721 droelectric_Energy_Storage_in_South_Africa_using_Aquifers_and_Existing_Infr
722 astructure (accessed 3.12.17).
723 Kipp, K., 1987. HST3D; a Computer Code for Simulation of Heat and Solute Transport in
724 Three-dimensional Ground-water Flow Systems. Government Documents.
725 Kipp, K.L., 1997. Guideto the Revised Heat and Solute Transport Simulator: HST3D
726 Version 2.
727 Koch, D. L., 1987. Iowa Geology 1987. Geological Survey Bureau / Iowa Deparment of
728 Natural Resources. Iowa
729 Kucukali, S., 2014. Finding the most suitable existing hydropower reservoirs for the
730 development of pumped-storage schemes: An integrated approach. Renewable
731 and Sustainable Energy Reviews 37, 502–508. doi:10.1016/j.rser.2014.05.052
732 Luick, H., Niemann, A., Perau, E., Schreiber, U., 2012. Coalmines as Underground
733 Pumped Storage Power Plants (UPP) - A Contribution to a Sustainable Energy
734 Supply? Presented at the EGU General Assembly Conference Abstracts, p. 4205.
735 Mason, I.G., 2015. Comparative impacts of wind and photovoltaic generation on energy
736 storage for small islanded electricity systems. Renewable Energy 80, 793–805.
737 doi:10.1016/j.renene.2015.02.040
738 Menéndez, J., Loredo, J., Fernandez, J. M., Galdo, M., 2017. Underground pumped-
739 storage hydro power plants with mine water in abandoned coal mines in northern
740 Spain. – In: Wolkersdorfer, C.; Sartz, L.; Sillanpää, M. & Häkkinen, A.: Mine Water
741 & Circular Economy (Vol I). – p. 6 – 14; Lappeenranta, Finland (Lappeenranta
742 University of Technology).
743 Mileva, A., Johnston, J., Nelson, J.H., Kammen, D.M., 2016. Power system balancing for
744 deep decarbonization of the electricity sector. Applied Energy 162, 1001–1009.
745 doi:10.1016/j.apenergy.2015.10.180
746 Mueller, S.C., Sandner, P.G., Welpe, I.M., 2015. Monitoring innovation in electrochemical
747 energy storage technologies: A patent-based approach. Applied Energy 137, 537–
748 544. doi:10.1016/j.apenergy.2014.06.082

749 Okazaki, T., Shirai, Y., Nakamura, T., 2015. Concept study of wind power utilizing direct
750 thermal energy conversion and thermal energy storage. Renewable Energy 83,
751 332–338. doi:10.1016/j.renene.2015.04.027
752 Parkhurst, D.L., 1995. User's quide to PHREEQE—a computer program for speciation,
753 reaction-path, advective transport, and inverse geochemical calculations. US
754 Geological Survey WatereResources graphical user interface for the geochemical
755 computer program Investigations Report.
756 Parkhurst, D.L., Appelo, C.A.J., 1999. User's guide to PHREEQC (Version 2): A computer
757 program for speciation, batch-reaction, one-dimensional transport, and inverse
758 geochemical calculations.
759 Parkhurst, D.L., Engesgaard, P., Kipp, K.L., 1995. Coupling the geochemical model
760 PHREEQC with a 3D multi-component solute transport model. Presented at the
761 Fifth Annual V.M. Goldschmidt Conference, Geochemical Society, Penn State
762 University, University Park, USA.
763 Parkhurst, D.L., Kipp, K.L., 2002. Parallel processing for PHAST: a three-dimensional
764 reactive-transport simulator, in: S. Majid Hassanizadeh, R.J.S., William G. Gray
765 and George F. Pinder (Ed.), Developments in Water Science, Computational
766 Methods in Water ResourcesProceedings of the XIVth International Conference
767 on Computational Methods in Water Resources (CMWR XIV). Elsevier, pp. 711–
768 718. doi:10.1016/S0167-5648(02)80128-9
769 Parkhurst, D.L., Kipp, K.L., Charlton, S.R., 2010. PHAST Version 2—A Program for
770 Simulating Groundwater Flow, Solute Transport, and Multicomponent
771 Geochemical Reactions: U.S. Geological Survey Techniques and Methods 6–A35.
772 Plummer, L.N., Wigley, T.M.L., Parkhurst, D.L., 1978. The kinetics of calcite dissolution
773 in CO 2 -water systems at 5 degrees to 60 degrees C and 0.0 to 1.0 atm CO 2.
774 Am J Sci 278, 179–216. doi:10.2475/ajs.278.2.179
775 Poulain, A., goderniaux, P., de dreuzy, J.-R., 2016. Study of groundwater-quarry
776 interactions in the context of energy storage systems. Presented at the EGU
777 General Assembly Conference Abstracts, p. 9055.
778 Price, W.A., Morin, K. and Hutt, N. (1997b), *Guidelines for the Prediction of Acid Rock*
779 *Drainage and Metal Leaching for Mines in British Columbia: Part II -*
780 *Recommended Procedures for Static and Kinetic Testing*, Proc. 4th International
781 Conference on Acid Rock Drainage, Vancouver, BC, p15-30.
782 Pujades, E., Orban, P., Bodeux, S., Archambeau, P., Erpicum, S., Dassargues, A.,
783 2017a. Underground pumped storage hydropower plants using open pit mines:

How do groundwater exchanges influence the efficiency? Applied Energy 190, 135–146. doi:10.1016/j.apenergy.2016.12.093

Pujades, E., Orban, P., Jurado, A., Ayora, C., Brouyère, S., Dassargues, A., 2017b. Water chemical evolution in Underground Pumped Storage Hydropower plants and induced consequences. Energy Procedia. Accepted.

Pujades, E., Willems, T., Bodeux, S., Orban, P., Dassargues, A., 2016. Underground pumped storage hydroelectricity using abandoned works (deep mines or open pits) and the impact on groundwater flow. Hydrogeology Journal 24, 1531–1546. doi:10.1007/s10040-016-1413-z

Robb, G.A., 1994. Environmental Consequences of Coal Mine Closure. The Geographical Journal 160, 33–40. doi:10.2307/3060139

Sánchez-España, J., Yusta, I., Diez-Ercilla, M., 2011. Schwertmannite and hydrobasaluminite: A re-evaluation of their solubility and control on the iron and aluminium concentration in acidic pit lakes. Applied Geochemistry 26, 1752–1774. doi:10.1016/j.apgeochem.2011.06.020

Sanz, E., Ayora, C., Carrera, J., 2011. Calcite dissolution by mixing waters: geochemical modeling and flow-through experiments. Geologica Acta 9, 67–77. doi:10.1344/105.000001652

Severson, M.J., 2011. Preliminary Evaluation of Establishing an Underground Taconite Mine, to be Used Later as a Lower Reservoir in a Pumped Hydro Energy Storage Facility, on the Mesabi Iron Range, Minnesota.

Sharma, P., Vyas, S., N, S.S., V, M.N., Rustagi, A., N, S., Ratnam, M., 2011. Acid mine discharge – Challenges met in a hydro power project.

Sharma, S., Sack, A., Adams, J.P., Vesper, D.J., Capo, R.C., Hartsock, A. and Edenborn, H.M., 2013. Isotopic evidence of enhanced carbonate dissolution at a coal mine drainage site in Allegheny County, Pennsylvania, USA. *Applied geochemistry*, *29*, pp.32-42.

Schlömer S., T. Bruckner, L. Fulton, E. Hertwich, A. McKinnon, D. Perczyk, J. Roy, R. Schaeffer, R. Sims, P. Smith, and R. Wiser, 2014: Annex III: Technology-specific cost and performance parameters. In: Climate Change 2014: Mitigation of Climate Change. Contribution of Working Group III to the Fifth Assessment Report of the Intergovernmental Panel on Climate Change [Edenhofer, O., R. Pichs-Madruga, Y. Sokona, E. Farahani, S. Kadner, K. Seyboth, A. Adler, I. Baum, S. Brunner, P. Eickemeier, B. Kriemann, J. Savolainen, S. Schlömer, C. von Stechow, T. Zwickel

and J.C. Minx (eds.)]. Cambridge University Press, Cambridge, United Kingdom and New York, NY, USA.

Spriet, J., 2014. A Feasibility study of pumped hydropower energy storage systems in underground cavities.

Steffen, B., 2012. Prospects for pumped-hydro storage in Germany. Energy Policy 45, 420–429. doi:10.1016/j.enpol.2012.02.052

Sterpejkowicz-Wersocki, W., 2014. Problem of Clogging in Drainage Systems in the Examples of the Żur and Podgaje Dams. Archives of Hydro-Engineering and Environmental Mechanics 61, 183–192. doi:10.1515/heem-2015-0012

Meyer, F., 2013. Storing wind energy underground. Publisher: FIZ Karlsruhe – Leibnz Institute for information infrastructure, Eggenstein Leopoldshafen, Germany. ISSN: 0937-8367.

Uddin, N., Asce, M., 2003. Preliminary design of an underground reservoir for pumped storage. Geotechnical and Geological Engineering 21, 331–355. doi:10.1023/B:GEGE.0000006058.79137.e2

Van Rossum G., Drake, F.L., 2011. The Python Language Reference Manual. Network Theory Ltd.

Water Framework Directive, Water Framework Directive, 2000/60/EC. Eur. Commun. Off. J., L327.22.12.2000.

White A.F., Brantley S.L., 1995. Chemical weathering rates of silicate mienrals: an overview. Reviews in Mineralogy, 31: 1-21.

Williamson, M.A. and Rimstidt, J.D., 1994. The kinetics and electrochemical rate-determining step of aqueous pyrite oxidation. Geochimica et Cosmochimica Acta, 58(24), pp.5443-5454.

Winde, F., Kaiser, F., Erasmus, E., 2017. Exploring the use of deep level gold mines in South Africa for underground pumped hydroelectric energy storage schemes. Renewable and Sustainable Energy Reviews 78, 668-682.

Wong, I.H., 1996. An underground pumped storage scheme in the Bukit Timah Granite of Singapore. Tunnelling and Underground Space Technology 11, 485–489. doi:10.1016/S0886-7798(96)00035-1

Xu, K., Dai, G., Duan, Z. and Xue, X., 2018. Hydrogeochemical evolution of an Ordovician limestone aquifer influenced by coal mining: a case study in the Hancheng mining area, China. *Mine Water and the Environment*, pp.1-11.

Younger, P.L., Banwart, S.A., Hedin, R.S., 2002. Mine Water: Hydrology, Pollution, Remediation. Springer Science & Business Media.

853 Zhang, N., Lu, X., McElroy, M.B., Nielsen, C.P., Chen, X., Deng, Y., Kang, C., 2016.
854 Reducing curtailment of wind electricity in China by employing electric boilers for
855 heat and pumped hydro for energy storage. Applied Energy 184, 987–994.
856 doi:10.1016/j.apenergy.2015.10.147.
857 Zillmann, A., Perau, E., 2015. A conceptual analysis for an underground pumped storage
858 plant in rock mass of the Ruhr region. Geotechnical Engineering for Infrastructure
859 and Development, pp. 3789-3794. Doi: 10.1680/ecsmge.60678.vol7.597.
860

Figure captions

Figure 1. General view of the problem. An underground reservoir (cavity) of 50 m by 50 m on 10 m height is considered. It is located below the water table.

Figure 2. a) Schematic view of the model domain. Half of the problem is modelled by taking advantage of its symmetry. b) View of the meshed numerical model.

Figure 3. pH evolutions in the surface (black continuous line) and underground (double continuous grey line) reservoirs and in the surrounding porous medium at the distances of 5 (dotted line) and 15 m (dashed line). The results are shown for both scenarios (Sce1 on the left and Sce2 on the right) under the hypotheses H1 (Figure 3a), H2 (Figure 3b) and H3 (Figure 3c).

Figure 4. Computed mass of the precipitated minerals in the surface reservoir during the simulated time. The results are shown for both scenarios (Sce1 on the left and Sce2 on the right) under hypotheses H1 (figure 4a), H2 (Figure 4b) and H3 (Figure 4c).

Figure 5. Percentage evolution of the dissolved minerals in the surrounding porous medium at 5 m from the underground reservoir. The results are shown for Sce1 (atmosphere-water equilibrium) and Sce2 (no equilibrium) under hypotheses H1 (Figure 5a), H2 (Figure 5b) and H3 (Figure 5c).

Figure 6. CO_2 emissions from the surface reservoir to the atmosphere. The results are shown for Sce1 (atmosphere-water equilibrium) and Sce2 (no equilibrium) under hypotheses H2 (top) and H3 (bottom).

Figures

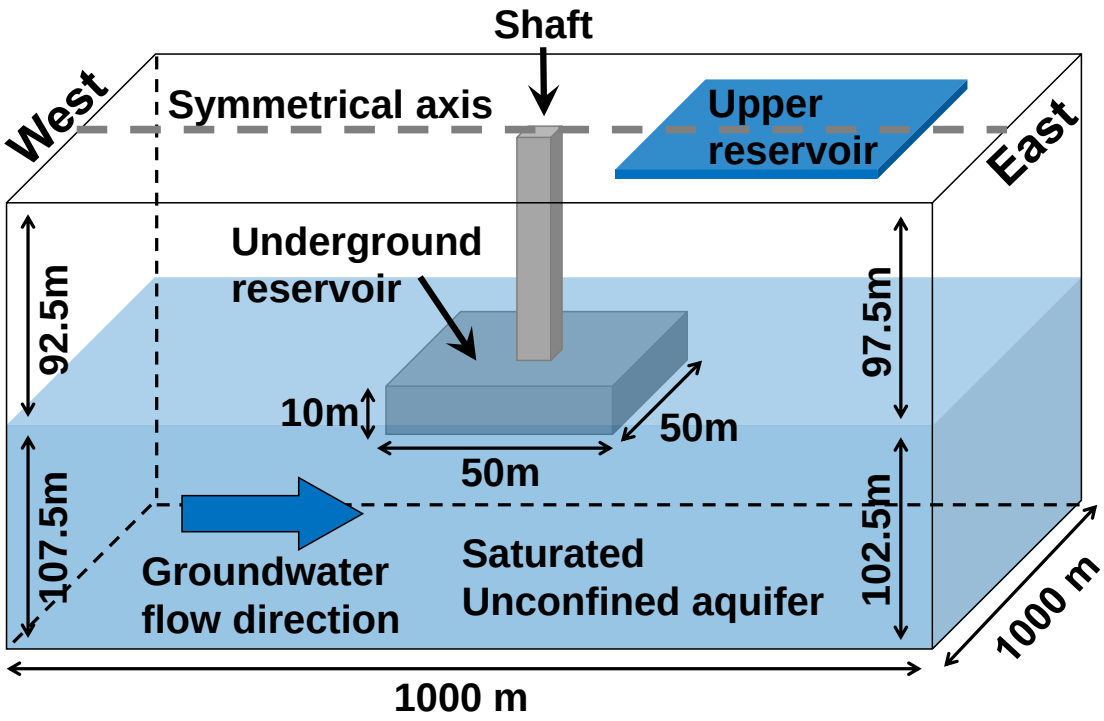

Figure 1

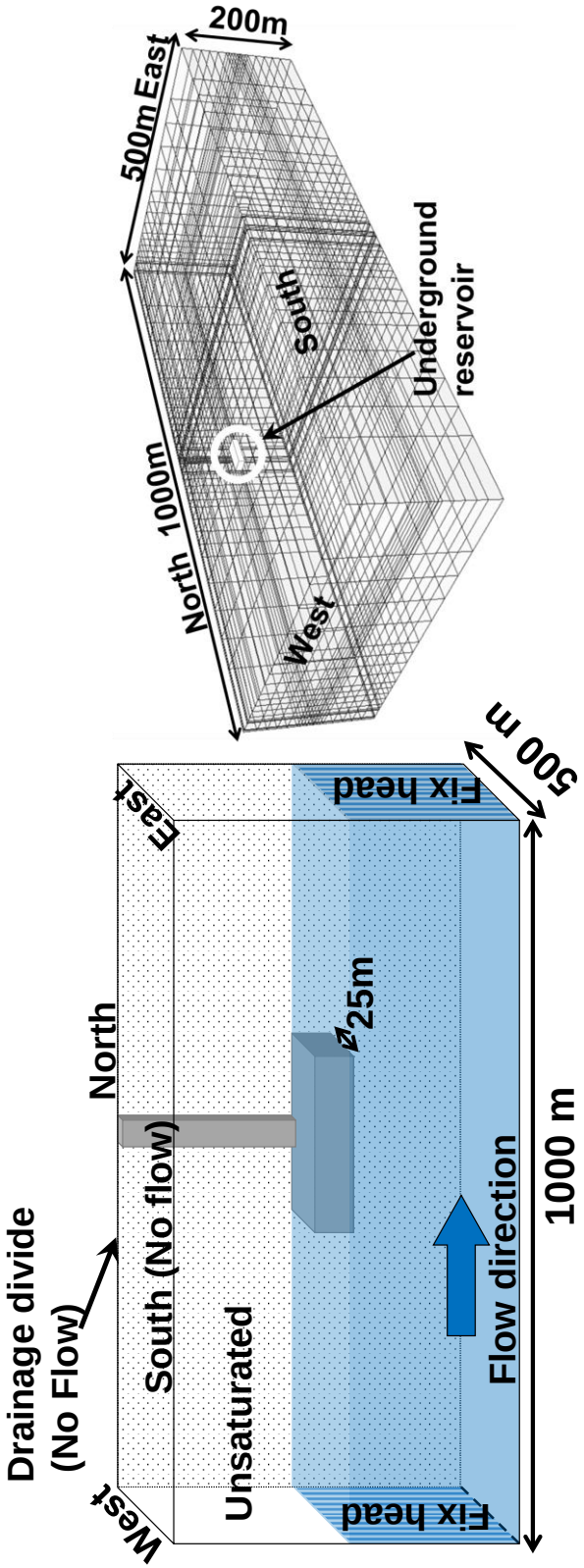
200m
500m East
South
Underground reservoir
North 1000m
West
500 m
Fix head
East
North
25m
1000 m
Drainage divide (No Flow)
South (No flow)
Unsaturated
Flow direction
West
Fix head

Figure 2

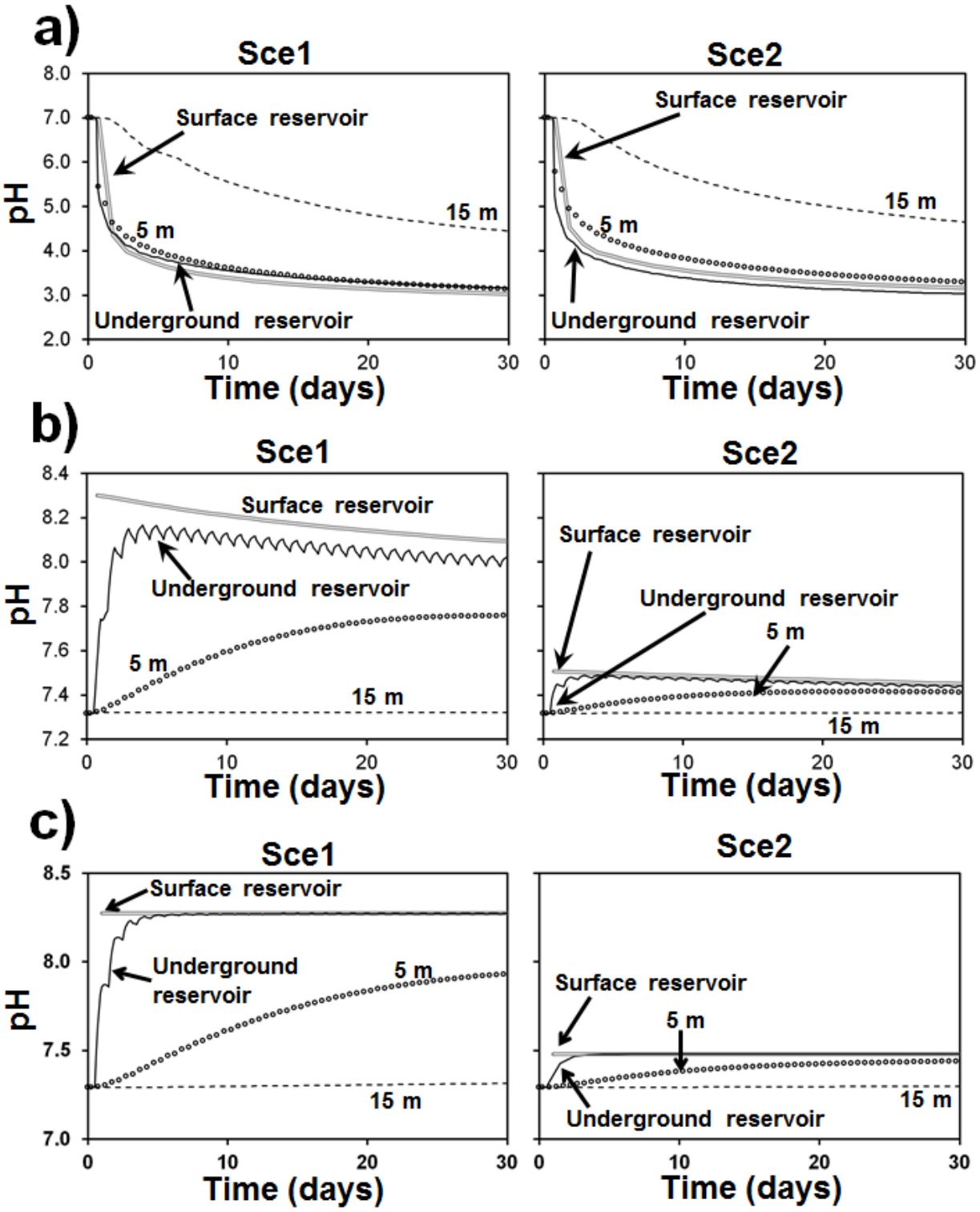
a)
Sce1
Sce2
Surface reservoir
15 m
5 m
Underground reservoir
pH
Time (days)
b)
Sce1
Sce2
Surface reservoir
Underground reservoir
5 m
15 m
pH
Time (days)
c)
Sce1
Sce2
Surface reservoir
Underground reservoir
5 m
15 m
pH
Time (days)

Figure 3

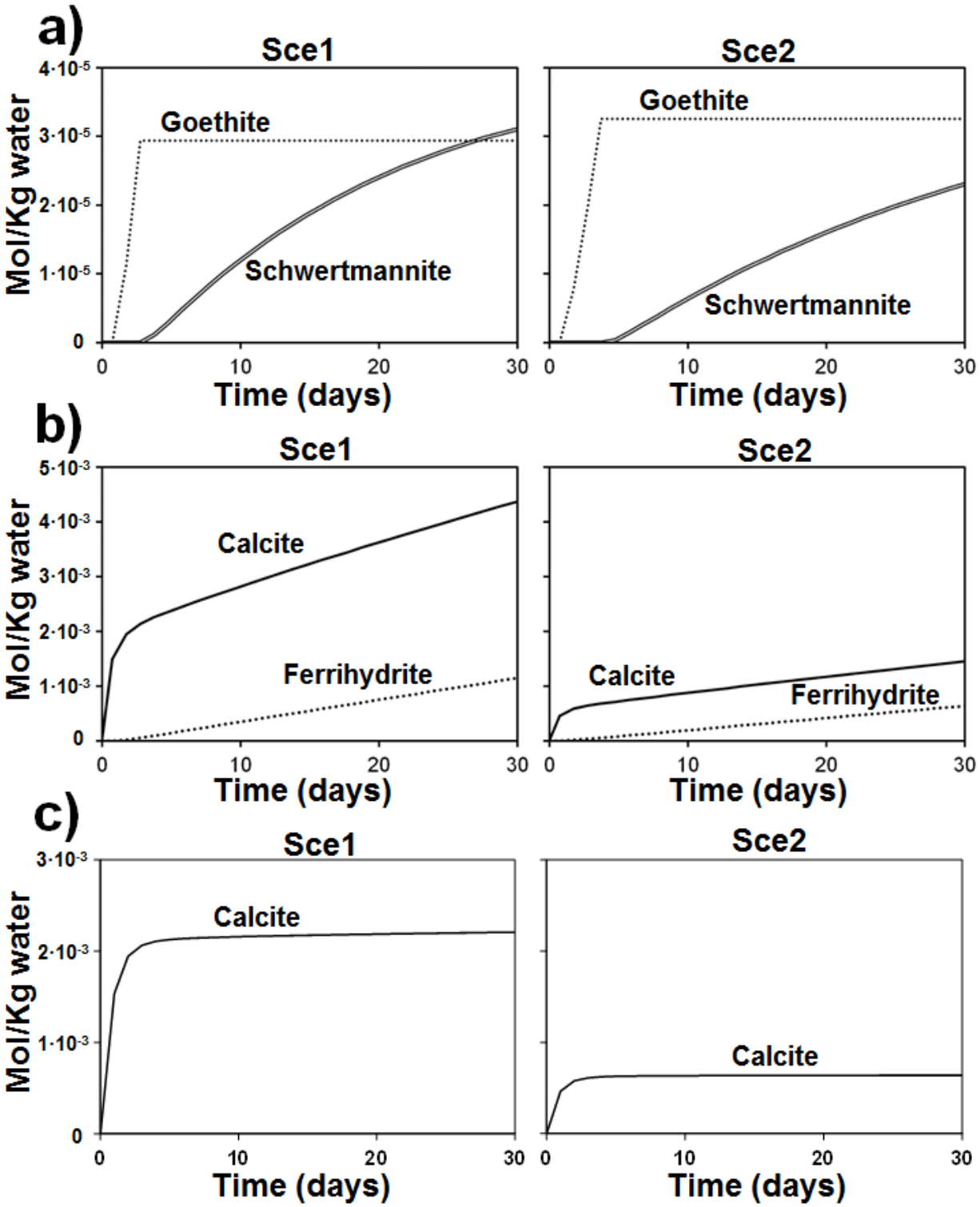
a)
Sce1
Sce2
Goethite
Schwertmannite
Mol/Kg water
4·10-5
3·10-5
2·10-5
1·10-5
0
0
10
20
30
Time (days)
b)
Calcite
Ferrihydrite
5·10-3
4·10-3
3·10-3
2·10-3
1·10-3
c)

Figure 4

Figure 5

Figure 6

Table captions

Table 1. Released CO_2 (g/kWh) generated. The results are obtained under hypotheses H2 and H3 considering the total CO_2 released during the simulated time and the volume of CO_2 released once the emission rates stabilize (≈after 10 days).

Tables

Hypothesis H2	Sce1 (g of CO2 per kWh)	Sce2 (g of CO2 per kWh)
Total CO_2 released	28	13
CO2 released after stabilization	15	9

Hypothesis H3	Sce1 (g of CO2 per kWh)	Sce2 (g of CO2 per kWh)
Total CO_2 released	14	5
CO2 released after stabilization	0.42	0.052

Table 1

Appendix A

This appendix shows the results of a sensitivity analysis in which the specific surface area (SSA) of the pyrite and the volume of pumped/discharged water are modified. Note that the effects of modifying the volume of the pumped/discharged water are analogous to those induced by the modification of the size of the underground reservoir. Results of Sce3 and Sce4 are compared with those obtained for Sce1. The SSA of pyrite is reduced one order of magnitude at Sce3 while the volume of pumped/discharged water is reduced in half at Sce4. Figure A2.1 and figure A2.2 display results for hypotheses H1 and H2, respectively. Note that, hypotheses H3 is not considered because significant results were not observed when the SSA of calcite was reduced. In fact, computed results considering kinetics of calcite were very similar to those obtained considering chemical equilibrium of calcite because its reaction rate is fast in comparison with our time scale. Concerning the volume of pumped/discharged water, the expected behavior is similar to that obtained for hypothesis H2. The main conclusions of this sensitivity analysis are that 1) trends are the same, 2) the behavior is slightly modified, and 3) the impacts of modifying the SSA and the volume of pumped/discharged water are similar for both considered hypotheses. Main changes are described below.

Hypothesis H1:

pH in the reservoirs (Figures A2.1 a and b) increases when the SSA of pyrite is reduced because less pyrite is dissolved in the surrounding porous medium and less protons are released. Larger mineral precipitations (per Kg of water) of goethite and schwertmannite are observed in Sce4 (Figure A2.1 c). Discharged water is more time in contact with the rock because the underground reservoir is not totally emptied and filled in Sce4, which may explain that more dissolved minerals are available to precipitate in the surface reservoir. Obviously, schwertmannite precipitation decreases for Sce3 since less pyrite is dissolved. Little differences are observed concerning the pH at the surrounding porous medium (5 m from the underground reservoir) (Figure A2.1 d). The most remarkable aspect is that pH increases when the SSA and the pumped/discharged volume of water are reduced. Finally, the evolution of the concentration of pyrite at the surrounding medium is displayed at 5 m (Figure A2.1 e) and 1 m (Figure A2.1 f) from

the underground reservoir. Apparently, more pyrite is dissolved at 5 m when the SSA is dissolved. However, this occurs because much less pyrite is dissolved in Sce3 near the underground reservoir (1 m) and more oxygen is available at 5 m. In Sce4, the dissolved pyrite is similar to that dissolved in Sce1 at 1 m whilst is much lower at 5 m because less discharged water reach this location. Globally, the volume of dissolved pyrite decrease for scenarios Sce3 and 4.

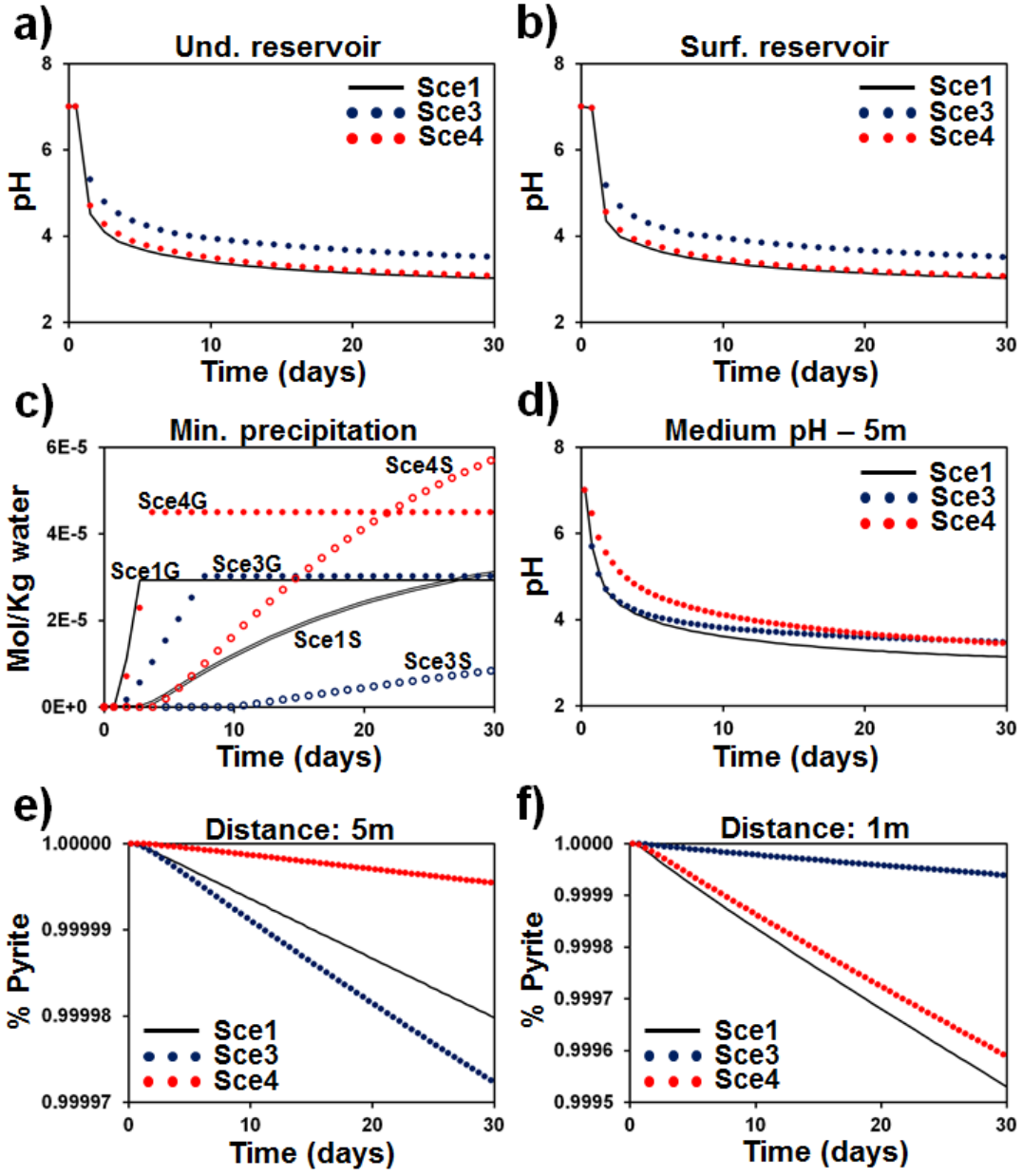

Figure A2.1. Results obtained for the scenarios Sce1, Sce3 and Sce4. This results allow determining the effects of reducing the SSA (Sce3) and the volume of pumped/discharged water (Sce4) when H1 is considered.

Hypothesis H2:

In general terms, the pH in the reservoirs (Figures A2.2 a and b) increases when the SSA and the volume of pumped/discharged water are decreased. The only exception is observed in the underground reservoir for Sce4. In this case, during early times the pH is lower than that computed for Sce1, after pH is equal for both scenarios. Mineral precipitations in the surface reservoir (Figure A2.1 c) increase when the volume of pumped/discharged water is reduced, while they decrease if the SSA is diminished because the dissolution of minerals in the surrounding porous medium is lowered. Concerning the pH evolution in the surrounding porous medium (Figure A2.1 d), the pH increases when the SSA is reduced because less pyrite is dissolved. In addition, the pH decreases when the volume of pumped/discharged water is reduced because the water exchanges between the underground reservoir and the surrounding porous medium are lowered. Consequently, the impact of the surrounding groundwater is smaller. Finally, as in the previous hypothesis, the mass of dissolved minerals decreases in Sce4 because the water exchanges are lowered. Moreover, it is also observed that the mass of dissolved minerals at 5 m increases when the SSA is reduced. This effect is produced because more reactants (dissolved oxygen) can reach this location since they are not previously consumed when the SSA is reduced. This fact is corroborated by the computed dissolutions at 1 m from the underground reservoir. At this location, much less minerals are dissolved for Sce3. In global terms, the volume of dissolved minerals decrease for scenarios Sce3 and Sce4.

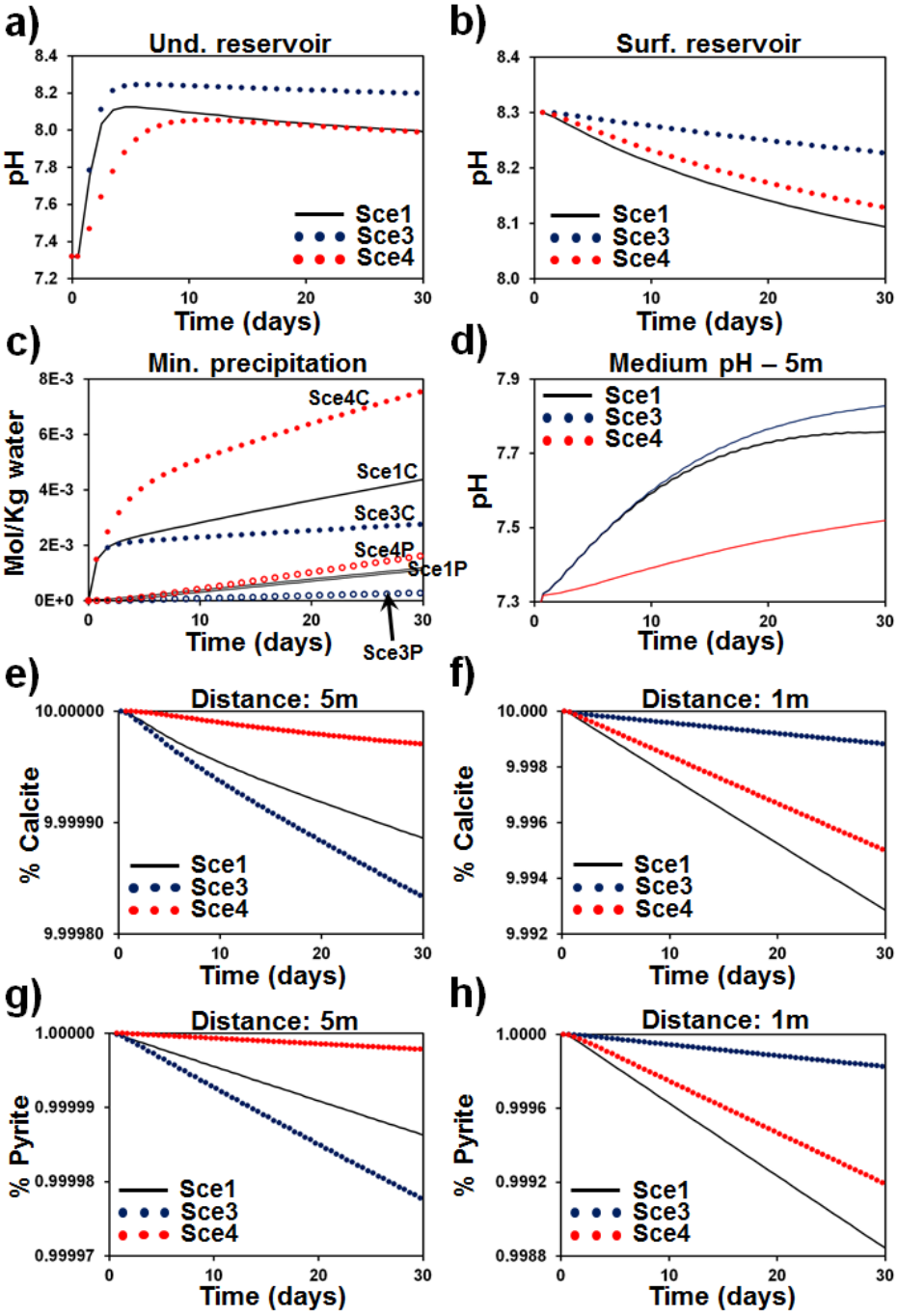

Figure A2.2. Results obtained for the scenarios Sce1, Sce3 and Sce4. This results allow determining the effects of reducing the SSA (Sce3) and the volume of pumped/discharged water (Sce4) when H2 is considered.

Appendix B

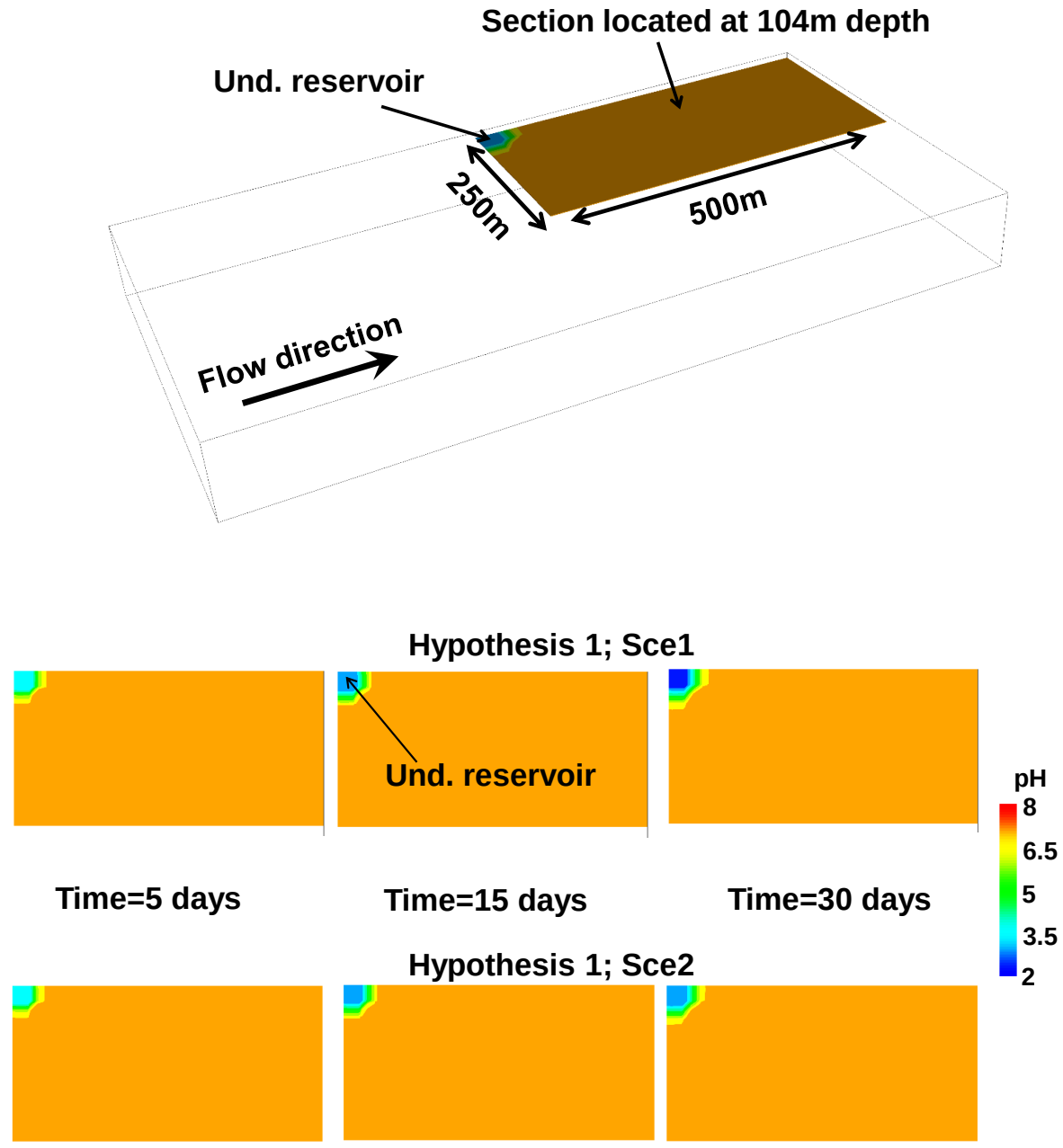

Figure A1. Computed pH distribution at 5, 15, and 30 days for scenarios Sce1 and Sce2 of hypothesis H1.

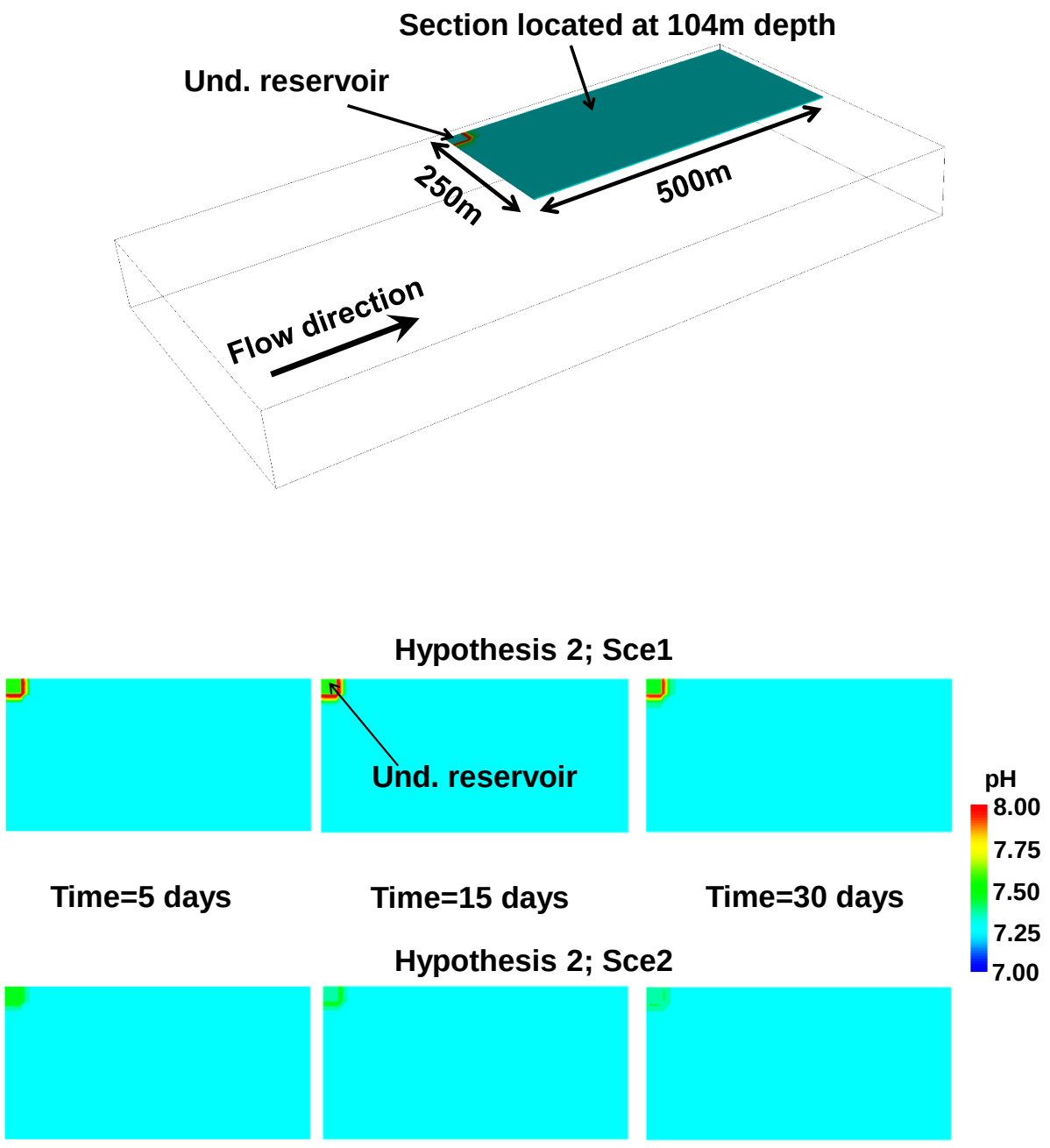

Figure A2. Computed pH distribution at 5, 15, and 30 days for scenarios Sce1 and Sce2 of hypothesis H2.

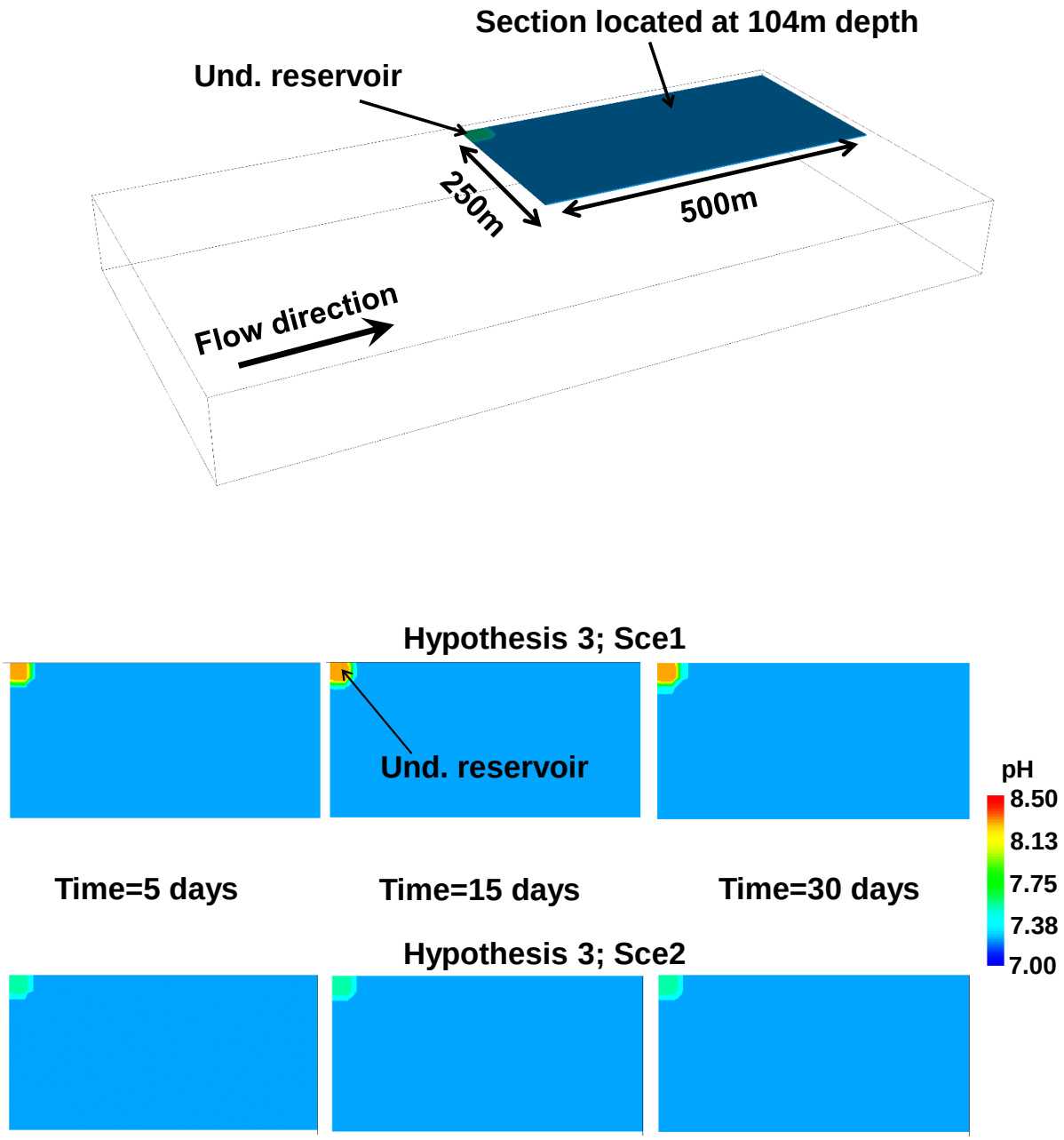

Figure A3. Computed pH distribution at 5, 15, and 30 days for scenarios Sce1 and Sce2 of hypothesis H3.